THE JOURNAL OF BIOLOGICAL CHEMISTRY
Vol. 277, No. 29, Issue of July 19, pp. 25992–26002, 2002

*Printed in U.S.A.*

# Evidence for Cooperativity between the Four Binding Sites of Dimeric ArsD, an As(III)-responsive Transcriptional Regulator*

Received for publication, February 18, 2002, and in revised form, April 26, 2002
Published, JBC Papers in Press, April 29, 2002, DOI 10.1074/jbc.M201619200

**Song Li‡, Barry P. Rosen‡, M. Ines Borges-Walmsley§, and Adrian R. Walmsley§¶**

*From the ‡Department of Biochemistry and Molecular Biology, Wayne State University School of Medicine, Detroit, Michigan 48201 and the §Division of Infection and Immunity, Institute of Biomedical and Life Sciences, The University of Glasgow, Glasgow G11 6NU, Scotland, United Kingdom*

**ArsD is a *trans*-acting repressor of the *arsRDABC* operon that confers resistance to arsenicals and antimonials in *Escherichia coli*. It possesses two-pairs of vicinal cysteine residues, $Cys^{12}$-$Cys^{13}$ and $Cys^{112}$-$Cys^{113}$, that potentially form separate binding sites for the metalloids that trigger dissociation of ArsD from the operon. However, as a homodimer it has four vicinal cysteine pairs. Titration of the steady-state fluorescence of ArsD with metalloids revealed positive cooperativity, with a Hill coefficient of 2, between these sites. Disruption of the $Cys^{112}$-$Cys^{113}$ site by mutagenesis of *arsD*, but not the $Cys^{12}$-$Cys^{13}$ site, largely abolished this cooperativity, indicative of interactions between adjacent $Cys^{112}$-$Cys^{113}$ sites within the dimer. The kinetics of metalloid binding were determined by stopped flow spectroscopy; the rate increased in a sigmoidal manner, with a Hill coefficient of 4, indicating that the pre-steady-state measurements reported cooperativity between all four sites of the dimer rather than just the intermolecular interactions reported by the steady-state measurements. The kinetics of Sb(III) displacement by As(III) revealed that the metalloid-binding sites behave differentially, with the rapid exchange of As(III) for Sb(III) at one site retarding the release of Sb(III) from the other sites. We propose a model involving the sequential binding and release of metalloids by the four binding sites of dimeric ArsD, with only one site releasing free metalloids.**

All cells possess regulatory mechanisms to tightly control the concentration of soft metals, including both essential metals, such as zinc and copper, and toxic metalloids, such as arsenite and antimony (1). A common homeostatic mechanism is the use of efflux systems, such as transport ATPases, to control the level of these soft metals in the cell. Failure of these regulatory systems can lead to genetic disorders, such as Menkes' disease and Wilson's disease in humans, caused by mutations in two Cu(I) pumps (2–6). Consequently, understanding the mechanism controlling the expression of these efflux pumps and the basis of their selectivity for toxic soft metals is of paramount importance. A common feature of the protein components of these regulatory systems is the use of pairs of cysteine residues to chelate the soft metals, with multiple copies of these soft metal-chelating sites occurring within each protein. However, there have been no transient kinetic studies, with the potential to define cooperative interactions, of metal or metalloid binding to such sites; consequently, the binding mechanism has not been elucidated, and our knowledge of the role played by the individual binding sites is still rudimentary.

High level resistance to arsenite and antimonite in *Escherichia coli* is conferred by the *arsRDABC* operon of plasmid R773 (7). The *arsA* and *arsB* genes encode the ATPase and membrane translocase subunits of an arsenical pump (8), whereas the *arsC* gene encodes an arsenate reductase that is required to catalyze the reduction of arsenate to arsenite prior to extrusion (9–13). The products of the *arsD* and *arsR* genes, which encode *trans*-acting repressors that bind to the *ars* operon, control the expression of the operon (14, 15). ArsR is a 117-residue protein that functions as a homodimer, repressing expression of the operon to a basal level in the absence of arsenite or antimonite, but in the presence of these metalloids it dissociates from the DNA, and transcription ensues. ArsD is also a homodimer of two 120-residue subunits that binds to the same operator site as ArsR but with an affinity that is 2 orders of magnitude less than that of ArsR. Consequently, ArsD only binds to the *ars* operon when produced in high concentrations, such as after prolonged stimulation of transcription of the *arsD* gene following induction by arsenite or antimonite. It has been proposed that ArsD controls the maximal level of expression of the operon, preventing the build-up of ArsB, which at high levels appears toxic to the cell (15). Although ArsD has an affinity for arsenite that is an order of magnitude lower than ArsR, at sufficiently high levels of arsenite, ArsD dissociates, and the operon is again transcribed. In both ArsR and ArsD vicinal pairs of cysteine residues have been shown to be involved in coordinating the metalloid (16, 17). The homodimeric ArsR has only a single metalloid blinding site/monomer, utilizing the $Cys^{32}$-$Cys^{34}$ pair to coordinate metalloids, whereas ArsD appears to have two, or four one-half metalloid-binding sites/monomer, utilizing the $Cys^{12}$-$Cys^{13}$ and $Cys^{112}$-$Cys^{113}$ pairs to coordinate metalloids. Substitution of either of these cysteine pairs in ArsD abolished metalloid inducibility but did not affect repression, indicating that these cysteine residues form metalloid-binding sites (17). The aim of the present study was to determine whether these sites are independent or whether they interact and to elucidate the mechanism of metalloid binding to these sites.

* This work was supported by grants from the Biotechnology and Biological Sciences Research Council and the Wellcome Trust (to A. R. W.), United States Public Health Service Grant AI45428 (to B. P. R.), and a Research Travel grant from the Burroughs Wellcome Fund, an award from the NATO Collaborative Research Grant Programme, and a Wellcome Trust Biomedical Research Collaboration grant (to A. R. W. and B. P. R.). The stopped flow instrument was purchased with grants from the University of Glasgow and the Royal Society. The costs of publication of this article were defrayed in part by the payment of page charges. This article must therefore be hereby marked "*advertisement*" in accordance with 18 U.S.C. Section 1734 solely to indicate this fact.

¶ To whom correspondence should be addressed: Div. of Infection and Immunity, Inst. of Biomedical and Life Sciences, Level 3, Robertson Bldg., University of Glasgow, 56 Dumbarton Rd., Glasgow G11 6NU, Scotland, UK. Tel.: 44-141-330-3750; Fax: 44-141-330-3750; E-mail: A.Walmsley@bio.gla.ac.uk.

## MATERIALS AND METHODS

*Purification of $His_6$-tagged ArsD*—ArsD and its derivatives were purified as described previously (17), quickly frozen, and stored in small aliquots at −80 °C. The concentrations of purified ArsD and its derivatives were determined using a Bio-Rad protein assay kit. An ArsD derivative in which the $Cys^{119}$ and $Cys^{120}$ residues were deleted and in which a $His_6$ tag was added to the C terminus was used as the basis for the construction of further derivatives in which the other cysteine residues were systematically changed to alanines.

*Fluorescence Measurements*—Fluorescence measurements were made in a Jasco FP750 fluorimeter at 20 °C. Tryptophan fluorescence was excited at 295 nm, and the emission wavelength was scanned between 300 and 400 nm. For titrations, Sb(III) was added as potassium antimonial tartrate from 1, 10, or 100 mM stock solutions to 2 ml of 1 μM ArsD protein (in 50 mM MOPS-KOH,[1] pH 7.5, 0.25 mM EDTA), so that the original sample was not diluted by more than 10%. The protein fluorescence and the Sb(III) concentration were corrected for the dilution effect.

Time-resolved fluorescence measurements were also carried out in an Applied Photophysics (London, UK) SX.18MV stopped flow instrument operated at 20 °C. For measurements of the change in tryptophan fluorescence, the samples were excited with light at 295 nm and selected with a monochromator, and the emission was monitored at wavelengths above 335 nm using a cut-off filter. Routinely, equal volumes of the reactants were mixed together in the stopped flow instrument, using two syringes of equal volume. The concentration of ArsD was 1 μM, unless otherwise noted, in 50 mM MOPS-KOH, pH 7.5, 0.25 mM EDTA. All of the concentrations are for the mixing chamber unless stated otherwise, so that the concentrations in the syringe were twice those quoted for the mixing chamber. To set up the stopped flow instrument, 1 μM ArsD protein was mixed with buffer, and the photomultiplier tube voltage was increased until a 4 V signal was achieved. Fluorescence changes were recorded as an increase or decrease in this 4 V signal (*i.e.* an increase in the signal from 4 to 4.1 V would correspond to a 2.5% increase in fluorescence and a decrease from 4 to 3.9 V would correspond to a 2.5% quench in fluorescence), which was backed off to zero, and changes above and below this zero base line were recorded.

*Data Analysis*—Stopped flow traces were analyzed by fitting to single ($s = A{\cdot}\exp^{-kt}$; where $s$ represents the change in signal (*e.g.* volts or percentage of fluorescence), $t$ represents the time, and $A$ and $k$ represent the amplitude and rate constant for the signal change, respectively) or multiple exponential functions ($s = A_1{\cdot}\exp^{-k(1)t} + A_2{\cdot}\exp^{-k(2)t} + A_3{\cdot}\exp^{-k(3)t}$, for a triple exponential function) using the nonlinear regression software with the Applied Photophysics stopped flow. Concentration dependence data were analyzed by nonlinear regression fitting to sigmoidal or hyperbolic functions, as required, using Sigmaplot 4.0. Drug titration curves were fitted to a sigmoidal function by nonlinear regression using the program Sigma Plot from Jandel Scientific.

$$\Delta F = \Delta F_{max} \cdot [Sb(III)]^n / K_{1/2}^n + [Sb(III)]^n \quad \text{(Eq. 1)}$$

where $\Delta F$ is the quench in protein fluorescence, $\Delta F_{max}$ is the maximum fluorescence quench, $K_{1/2}$ is the half-saturation constant, and $n$ is the Hill coefficient.

## RESULTS

*The Steady-state Kinetics of Sb(III) and As(III) Binding to ArsD*—The binding of Sb(III) and As(III) to ArsD induces a quench in the protein fluorescence (17) that was used to titrate the ArsD metalloid-binding site. ArsD contains only two tryptophan residues, $Trp^{35}$ and $Trp^{97}$, of which only the latter contributes to metalloid responsiveness. In a previous study we established that although the vicinal cysteine pair $Cys^{119}$-$Cys^{120}$ could bind metalloids, it did not have an apparent effect on repression or metalloid responsiveness *in vivo* or *in vitro* (17). Accordingly, to avoid complications in the interpretation of the data for the binding of Sb(III) to ArsD and to provide the base-line data for our study, we produced and characterized a C-terminal His-tagged $Cys^{119}$-$Cys^{120}$ deletion derivative of ArsD, which, for simplicity, we refer to as ArsD throughout the manuscript and into which further amino acid substitutions were introduced. The titration curves for the binding of Sb(III) and As(III) to 1 μM of ArsD (*i.e.* the $Cys^{119}$-$Cys^{120}$ deletion derivative) indicated that binding is a cooperative process (Fig. 1) and was characterized by Hill coefficients of 2.1 ± 0.2 and 2.1 ± 0.1 and maximal quenches in the protein fluorescence of 56 ± 1 and 26 ± 1% for Sb(III) and As(III), respectively. However, the titration curve for Sb(III) was to the left of that for As(III), with $K_{1/2}$ values of 1.7 ± 0.6 and 11.2 ± 4.5 μM, respectively, indicating that ArsD has higher affinity for Sb(III) than As(III). Comparatively, the His-tagged wild type protein (termed wild type ArsD), which possessed the $Cys^{119}$ and $Cys^{120}$ residues, behaved in an identical manner (Table I).

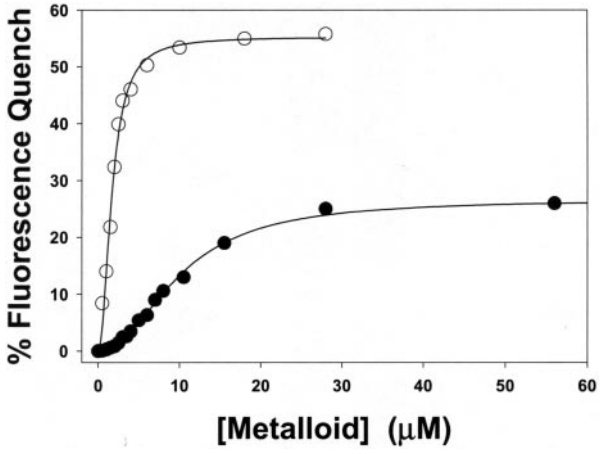


FIG. 1. **Steady-state titration of ArsD protein fluorescence with Sb(III) and As(III).** The protein fluorescence (excitation = 295 nm, emission = 300–450 nm) of 1 μM ArsD was titrated with Sb(III) (○) or As(III) (●), by making microliter additions from 1 and 10 mM stock solutions so as to maintain the dilution effect to less than 10%. The data are plotted as the percentages of quench in the initial fluorescence of unliganded ArsD as a function of the added Sb(III) or As(III) concentration. The *smooth curve* through each trace is the best fits to a sigmoidal equation with a Hill coefficient of 2.1 ± 0.2 and 2.1 ± 0.1, and maximal quenches in the protein fluorescence of 45 ± 1% and 20 ± 1% for Sb(III) and As(III), respectively.

*Evidence for Cooperativity between Adjacent Protomers of Dimeric ArsD*—To investigate the molecular basis of the cooperative interactions between the metalloid-responsive binding sites of dimeric ArsD, $Cys^{12}$, $Cys^{13}$, $Cys^{112}$, and $Cys^{113}$ were systematically substituted by alanine residues to disrupt each potential binding site. Our previous studies suggested that the vicinal cysteine pairs $Cys^{12}$-$Cys^{13}$ and $Cys^{112}$-$Cys^{113}$ form separate metalloid-binding sites. As shown in Table I, disruption of the $Cys^{12}$-$Cys^{13}$ site by replacing either $Cys^{12}$, $Cys^{13}$, or both did not affect the cooperativity in the binding of Sb(III). In contrast, disruption of the $Cys^{112}$-$Cys^{113}$ site caused a major reduction in the binding cooperativity. This behavior indicates that the observed cooperativity probably does not arise from interactions between the $Cys^{12}$-$Cys^{13}$ and $Cys^{112}$-$Cys^{113}$ sites but more likely arises from interactions between $Cys^{112}$-$Cys^{113}$ sites of the dimer. Indeed, not only does disruption of the $Cys^{112}$-$Cys^{113}$ site reduce cooperativity but also causes a 75–80% reduction in the fluorescence response of the protein to the binding of Sb(III), suggesting that the changes in ArsD fluorescence are primarily reporting events at the $Cys^{112}$-$Cys^{113}$ site. Consequently, the titration curves for ArsD might only reflect filling of the two $Cys^{112}$-$Cys^{113}$ sites in dimeric ArsD, and cooperative interactions with the $Cys^{12}$-$Cys^{13}$ sites might go unobserved. It is important to note that although disruption of the $Cys^{112}$-$Cys^{113}$ sites dramatically reduces the cooperative effects, these are not totally abolished. For example, the Hill coefficient for C112A/C113A ArsD was 1.1. These data suggest

[1] The abbreviations used are: MOPS, 4-morpholinepropanesulfonic acid; DTT, dithiothreitol.

TABLE I
*Steady-state titration data for ArsD and its substitution derivatives*

| ArsD derivatives | Fluorescence quench | Hill coefficient |
|---|---|---|
| | % | |
| Native | | |
| Wild type ArsD (Sb)[a] | 52 ± 5 | 2.0 ± 0.2 |
| ArsD ($Cys^{119}$-$Cys^{120}$ deletion) (Sb) | 55 ± 5 | 2.2 ± 0.2 |
| ArsD ($Cys^{119}$-$Cys^{120}$ deletion) (As) | 26 ± 4 | 2.1 ± 0.2 |
| Single substitutions[b] | | |
| C12A | 52 ± 5 | 2.0 ± 0.2 |
| C13A | 57 ± 3 | 2.2 ± 0.2 |
| C112A | 14 ± 3 | 1.3 ± 0.2 |
| C113A | 17 ± 3 | 1.2 ± 0.2 |
| Double substitutions[b] | | |
| C12A/C13A | 52 ± 4 | 2.1 ± 0.2 |
| C112A/C113A | 11 ± 2 | 1.1 ± 0.1 |
| Triple and quadruple substitutions[b] | | |
| C12A/C13A/C112A | 13 ± 3 | $K_m$ = 417 ± 24 μM[c] |
| C12A/C13A/C112A/C113A | No response | |

[a] Wild-type ArsD bearing a C-terminal $His_6$ tag.
[b] ArsD Cys-Ala derivatives were constructed in the ArsD ($Cys^{119}$-$Cys^{120}$ deletion) derivative.
[c] The data was adequately fitted to a hyperbolic function.

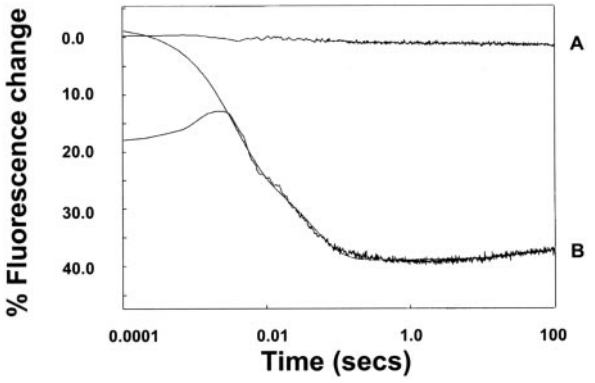


FIG. 2. **Sb(III)-induced conformational changes in ArsD.** Two semi-logarithmic plots of stopped flow traces generated by mixing 1 μM ArsD with buffer (*A*) and 120 μM Sb(III) (*B*). Changes in the ArsD fluorescence were recorded with excitation = 295 nm and emission > 335 nm. The *smooth curve* through *trace B* was the best fit to a triple-exponential function, with rate constants of 290 ± 6, 24 ± 2, and 0.003 ± 0.001 $s^{-1}$.

that there is cooperativity between the $Cys^{12}$-$Cys^{13}$ and $Cys^{112}$-$Cys^{113}$ sites in addition to that between the $Cys^{112}$-$Cys^{113}$ sites of the dimer. Interestingly, C12A/C13A/C112A ArsD was able to bind Sb(III), but in a noncooperative manner (*e.g.* $K_m$ = 417 + 24 μM; Table I), whereas C12A/C13A/C112A/C113A ArsD was optically unresponsive, presumably because it did not bind Sb(III). Because a vicinal cysteine pair is generally considered necessary to bind the metalloid or metal, this suggests that the binding sites are formed between the cysteine residues of adjacent monomers within the dimer.

*The Kinetics of the Formation of the ArsD-Sb(III) Complex*—We utilized the Sb(III)-induced quench in ArsD protein fluorescence to time resolve the interaction of Sb(III) with ArsD by stopped flow fluorescence spectroscopy. The stopped flow trace shown in Fig. 2, for the mixing of 1 μM ArsD with 120 μM Sb(III), indicates a multiphasic decrease in fluorescence over the first 10 s of the reaction, followed by a small increase in fluorescence over the next 90 s. When the reaction was studied over a longer time, it became apparent that the increase in fluorescence was transient and that it decreased over longer times (data not shown). The trace was best fitted to a triple-exponential function, with rate constants of 290 ± 6 $s^{-1}$ (phase 1; 59.5% of fluorescence quench), 24 ± 2 $s^{-1}$ (phase 2; 40.5% of fluorescence quench), and 0.003 ± 0.001 $s^{-1}$ (phase 3). It should be noted that phase 3 defines the small increase in fluorescence over the last 90 s of the trace and is attributed a "negative amplitude." As indicated in Fig. 2, there is a loss of amplitude because a large proportion of phase 1 occurs in the dead time of the stopped flow; the difference in the fluorescence of ArsD mixed with buffer (trace A) and 120 μM Sb(III) (trace B) is indicative of a 39% quench in the fluorescence of ArsD by 120 μM Sb(III), which is reasonably consistent with the maximal fluorescence quench determined in steady-state fluorescence titrations performed with the same protein preparation (*i.e.* this preparation gave a maximal steady-state quench of 45%). For lower concentrations of Sb(III), the stopped flow traces were adequately defined by a double-exponential function, without phase 3.

The dependence of the rate of each phase upon the Sb(III) concentration was investigated. The rates of phases 1 and 2 clearly increased in a sigmoidal manner (Fig. 3), whereas phase 3 had no significant dependence upon concentration, indicative of a conformational isomerization of the ArsD-Sb(III) complex (data not shown). The data for each phase were fitted to the following equation,[2]

$$\text{Rate} = k_{\min} + (k_{\max} \cdot [\text{Sb(III)}]^n)/(K_{1/2}^n + [\text{Sb(III)}]^n) \qquad \text{(Eq. 2)}$$

where $k_{\min}$ and $k_{\max}$ are the minimum and maximum rates of the conformational change induced by Sb(III) and $n$ is the Hill coefficient. For phase 1, this fitting procedure indicated values for the Hill coefficient, $K_{½}$, $k_{\max}$, and $k_{\min}$ of 4.0 ± 0.7, 45 ± 2 μM, 246 ± 14 $s^{-1}$, and 29 ± 9 $s^{-1}$, respectively (Fig. 3, *top panel*), whereas for phase 2, these constants had values of 3.7 ± 0.6, 44 ± 2 μM, 24 ± 1 $s^{-1}$, and 4.8 ± 0.8 $s^{-1}$, respectively (Fig. 3, *bottom panel*). The fact that the rates of both phase 1 and 2 are dependent upon the Sb(III) concentration suggests that ArsD has two nonidentical binding sites for Sb(III). Moreover, although the number of binding sites is not defined by the Hill coefficient, it does set a lower limit on the number of sites; there must be at least four interactive sites in functional ArsD to give a Hill coefficient of 4. The ArsD monomer has two binding sites for metalloids but forms dimers, and our data would be consistent with all of these sites interacting in a positive cooperative manner.

Interestingly, for concentrations of Sb(III) below 10 μM, there was a deviation away from the best fit curves in Fig. 3 for phases 1 and 2, with the rates of these phases dropping off

[2] Only the data points corresponding to concentrations above 10 μM were initially used for curve fitting.

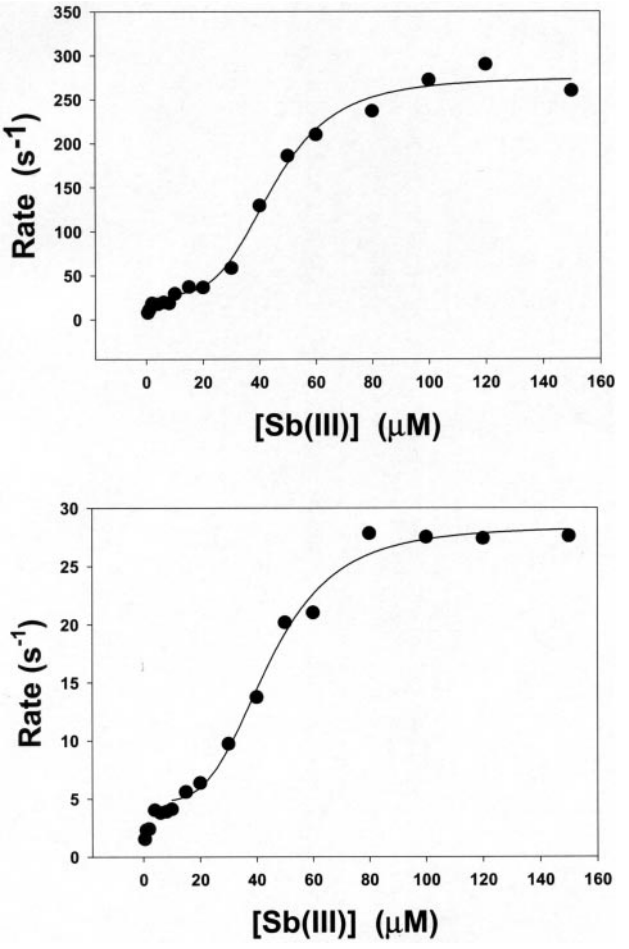


FIG. 3. **The Sb(III) concentration dependence of the rate of formation of the ArsD-Sb(III) complex.** A series of stopped flow records were generated by mixing 1 $\mu$M ArsD with Sb(III) at the indicated concentrations, in a stopped flow device. The rates of the fast (*top panel*) and intermediate (*bottom panel*) decrease in the fluorescence of ArsD induced by the binding of Sb(III) are plotted as a function of the Sb(III) concentration. Each rate constant increased in a sigmoidal manner, and the *curves* through the data points are the best fits to a sigmoidal equation (Equation 2), indicating values for the Hill coefficient, $K_{½}$, $k_{max}$, and $k_{min}$ of 4.0 ± 0.7, 45 ± 2 $\mu$M, 246 ±14 $s^{-1}$ and 29 ± 9 $s^{-1}$, and 3.7 ± 0.6, 44 ± 2 $\mu$M, 24 ± 1 $s^{-1}$, and 4.8 ± 0.8 $s^{-1}$ for the fast and intermediate phases, respectively.

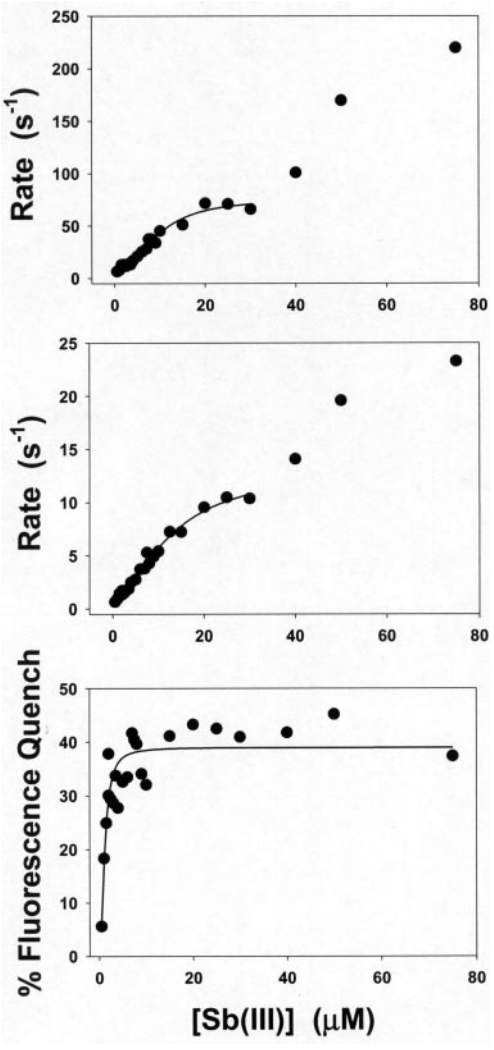


FIG. 4. **The Sb(III) concentration dependence of the rate and amplitude of the signal associated with formation of the ArsD-Sb(III) complex.** A series of stopped flow records were generated by mixing 1 $\mu$M ArsD with Sb(III) over a limited subsaturating concentration range of 0.5–75 $\mu$M Sb(III) in a stopped flow device. The rates of the fast (*top panel*) and intermediate (*middle panel*) decrease in the fluorescence of ArsD, induced by the binding of Sb(III), are plotted as a function of the Sb(III) concentration. Each rate constant increased in a sigmoidal manner, and the *curves* through the data points are the best fits to a sigmoidal equation (Equation 2), indicating values for the Hill coefficient, $K_{½}$, $k_{max}$, and $k_{min}$ of 2.2 ± 0.4, 9.8 ± 1 $\mu$M, 67 ± 7 $s^{-1}$, and 9.3 ± 2.0 $s^{-1}$, and 1.7 ± 0.3, 13 ± 2 $\mu$M, 12.3 ± 1.5 $s^{-1}$, and 0.9 ± 0.3 $s^{-1}$ for the fast and intermediate phases, respectively. In the *bottom panel*, the total signal amplitude (percentage of fluorescence quench) is shown as a function of the Sb(III). The *smooth curve* through the data points is the best fit to a sigmoidal equation, indicating a Hill coefficient of 2.0 ± 0.5 and a maximal quench of 39.0 ± 1.4%.

more rapidly than predicted. Accordingly, we reinvestigated this part of the titration curve, obtaining more data points between 0 and 50 $\mu$M Sb(III). As shown in Fig. 4 (*top panel*), over this concentration range the rate of phase 1 increased in an apparently sigmoidal manner with the Sb(III) concentration and was best fitted to Equation 2 with values for the Hill coefficient, $K_{½}$, $k_{max}$, and $k_{min}$ of 2.2 ± 0.4, 9.8 ± 1 $\mu$M, 67 ± 7 $s^{-1}$, and 9.3 ± 2.0, $s^{-1}$, respectively. Consistent with the data in Fig. 3, the rate increased more rapidly for concentrations above 40 $\mu$M. Phase 2 behaved in a parallel manner, indicating a Hill coefficient of 1.7 ± 0.3 (Fig. 4, *middle panel*). It is notable that this sigmoidal behavior occurs over the same concentration range as the steady-state titration curve for ArsD (Fig. 1), and, although the corresponding amplitude data were more variable than the steady-state measurements, the concentration dependence of the amplitude data (*e.g.* total percentage of fluorescence change) was best fitted to a sigmoidal function with a Hill coefficient of 2.0 ± 0.5 and a $\Delta F_{max}$ of 39 ± 1% (Fig. 4, *bottom panel*).

It is tempting to speculate that phases 1 and 2 correspond to the filling of the two metalloid-binding sites (*e.g.* $Cys^{12}$-$Cys^{13}$ and $Cys^{112}$-$Cys^{113}$, respectively) within the monomer. However, as noted above, the concentration dependence of each phase is characterized by two sigmoidal dependences, at low (0–20 $\mu$M) and high (20–150 $\mu$M) concentrations of Sb(III). Moreover, for each phase, the increase in rate over the higher concentration range was characterized by a Hill coefficient of about 4, indicating that all four sites of dimeric ArsD are involved. On the other hand, the steady-state titration curve indicated that ArsD approaches saturation with Sb(III) at 20 $\mu$M, suggesting that the high affinity (detected by steady-state measurements) and the low affinity (detected by pre-steady-state measurements) ArsD-Sb(III) complexes are kinetically coupled; the latter is the initial ArsD-Sb(III) complex, and the former is the final ArsD-Sb(III) complex; these complexes are connected by a conformational change from one to the other. As

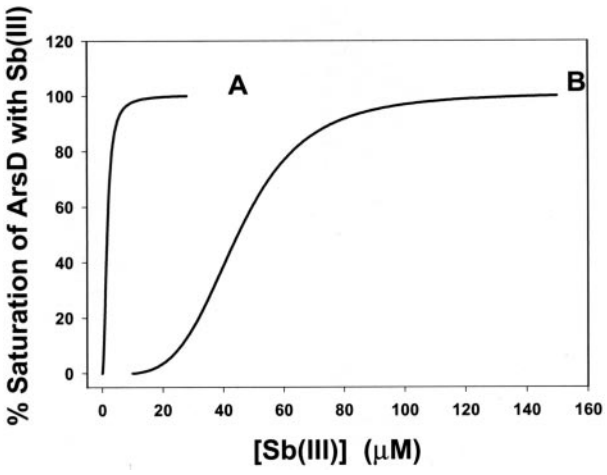


FIG. 5. **Percentage saturation curves for the formation of the initial and final ArsD-Sb(III) complexes.** The titration curves from Figs. 1 and 3 (*top panel*) were normalized to the maximal change. The curve for the initial ArsD-Sb(III) complex (*curve A*) is displaced to the right of that for the final ArsD-Sb(III) complex (*curve B*), indicating that there is a further conformational change in the initial complex as it adopts the final complex in which the Sb(III) is bound more tightly.

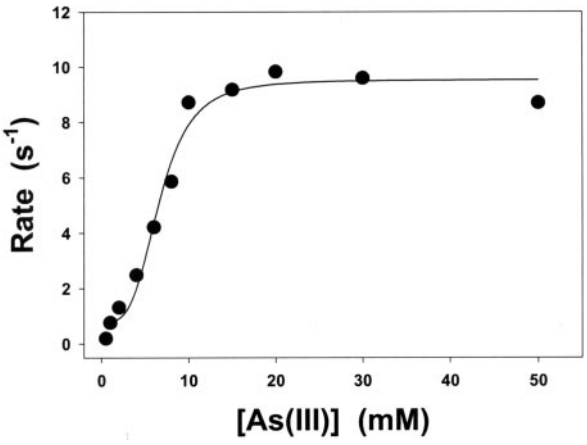


FIG. 6. **The As(III) concentration dependence of the rate of formation of the ArsD-As(III) complex.** A series of stopped flow records were generated by mixing 1 $\mu$M ArsD with As(III), at the indicated concentrations, in a stopped flow device. The rates of the fast decrease in the fluorescence of ArsD, induced by the binding of As(III), are plotted as a function of the As(III) concentration. The rate constant increased in a sigmoidal manner, and the *curve* through the data points is the best fit to a sigmoidal equation (Equation 2), indicating values for the Hill coefficient, $K_{½}$, $k_{max}$, and $k_{min}$ of 3.6 ± 0.8, 7 ± 1 $\mu$M, 8.7 ± 0.6 $s^{-1}$, and 0.8 ± 0.4 $s^{-1}$, respectively.

illustrated by Fig. 5, the titration curve for formation of the initial ArsD-Sb(III) complex, defined by the Sb(III) concentration dependence of the rate of binding of Sb(III) (*e.g.* either phase 1 or 2), is displaced to the right of the titration curve for the final ArsD-Sb(III) complex, defined by the Sb(III) concentration dependence of the steady-state fluorescence of ArsD, with half-saturation points for the initial and final complexes of about 44 and 1.7 $\mu$M, respectively. The simplest explanation for this behavior is that following the binding of Sb(III) to ArsD, the protein undergoes a conformational change that tightens the hold on Sb(III), probably in adopting a conformation that causes ArsD to dissociate from the *arsRDABC* promoter. Indeed, the equilibrium between these conformational states should be defined by $k_{max}$ and $k_{min}$ (*e.g.* forward and backward rate constants) determined for the binding of Sb(III) by the following relationship: $K_{final} = K_{initial}/(1 + k_{max}/k_{min})$, where $K_{initial}$ and $K_{final}$ are the half-saturation constants for the initial and final ArsD-Sb(III) complexes, respectively. Applying this relationship, with the values determined for phase 1 for $k_{max}$, $k_{min}$, and $K_{initial}$ of 246 $s^{-1}$, 29 $s^{-1}$, and 44 $\mu$M, respectively, gave a calculated value for $K_{final}$ of 4.6 $\mu$M. Although this value is slightly higher than the expected value of 1.7 $\mu$M, this difference could easily be accounted for by an additional conformational change that further tightens the binding. Indeed, we note that phase 2 is characterized by $k_{max}$ and $k_{min}$ values of 23.6 $s^{-1}$ and 4.8 $s^{-1}$, respectively, indicative of another conformational change that would yield a $K_{final}$ of 0.8 $\mu$M. There is still a remaining question as to what process is being measured at low Sb(III) concentrations (*i.e.* below 10 $\mu$M). Two possibilities are that 1) the measurements detect filling of the first two sites, which is necessary to "activate" ArsD so that it can undergo the conformational change to the final state or 2) a slow conformational change subsequent to formation of the initial ArsD-Sb(III) complex is being measured. The former scenario is more likely because this occurs with a Hill coefficient of 2, not 4, as would be expected for the latter scenario. Furthermore, the steady-state studies indicate that the fluorescence quench is largely attributable to the binding of metalloids to the $Cys^{112}$-$Cys^{113}$ site, and the measurements detect the filling of these sites within the dimer preferentially.

*The Kinetics of the Formation of the ArsD-As(III) Complex*—The stopped flow traces for the binding of As(III) to ArsD were biphasic, but only the rate of the fast phase, which accounted for about 90% of the signal amplitude, was dependent upon the As(III) concentration (data not shown). The rate of this fast phase increased in a sigmoidal manner with the As(III) concentration, and a fit of the data to Equation 2 indicated values for the Hill coefficient, $K_{½}$, $k_{max}$, and $k_{min}$ of 3.6 ± 0.8, 6.6 ± 0.5 mM, 8.7 ± 0.6 $s^{-1}$, and 0.8 ± 0.4 $s^{-1}$, respectively (Fig. 6). However, as noted for the binding of Sb(III) (Figs. 2 and 3), the first few data points deviated from the best fit sigmoidal curve. Thus, although a second concentration-dependent phase for As(III) was not observed, possibly because this is obscured by the lower signal amplitude, As(III) behaves in a manner similar to that of Sb(III). These data confirm the cooperative binding of metalloids by all four binding sites of dimeric ArsD but indicate that the conformational change from the initial to the final ArsD-As(III) complex occurs at a rate that is more than an order of magnitude slower than for Sb(III). Interestingly, there is a discrepancy between the calculated overall $K_{½}$ (*i.e.* $K_{final} = K_{initial}/(1 + k_{max}/k_{min})$ = 660 $\mu$M/(1 ± 8.7 $s^{-1}$/0.8 $s^{-1}$) = 54 $\mu$M) and that obtained from the steady-state titration curve (*e.g.* $K_{½}$ = 11.2 $\mu$M; Fig. 1); this is indicative of a further conformational change (*i.e.* the binding of As(III) to ArsD is at least a three-step process) that is rate-limiting.

*Dissociation of Sb(III) from the ArsD-Sb(III) Complex*—Dilution of the ArsD-Sb(III) complex with DTT to sequester the Sb(III) caused dissociation of the complex, as indicated by the increase in fluorescence of ArsD as the Sb(III) dissociated (Fig. 7), but no increase in protein fluorescence was observed when unliganded ArsD was mixed with DTT (data not shown). As expected, the ArsD-Sb(III) complex could not be dissociated by dilution with buffer in the stopped flow, because this only produced a drop in the Sb(III) concentration from 20 to 10 $\mu$M, which is still above the $K_{½}$; however, when 2 $\mu$M ArsD/5 $\mu$M Sb(III) was diluted 1:1 with buffer to drop the Sb(III) concentration below the $K_{1/2}$, the Sb(III) dissociated very slowly over several hours (data not shown). The stopped flow traces shown in Fig. 7 for the mixing of 1 $\mu$M ArsD/20 $\mu$M Sb(III) with 0.5 mM DTT (*trace A*) and 5 mM DTT (*trace B*) were best fitted to biphasic exponential equation with rate constants of 20.0 ± 0.2 $s^{-1}$ (86% of total signal amplitude) and 0.55 ± 0.02 $s^{-1}$ (14% of total signal amplitude) for *trace A* and 166 ± 3 $s^{-1}$ (90% of total signal amplitude) and 5.2 ± 0.2 $s^{-1}$ (10% of total signal ampli-

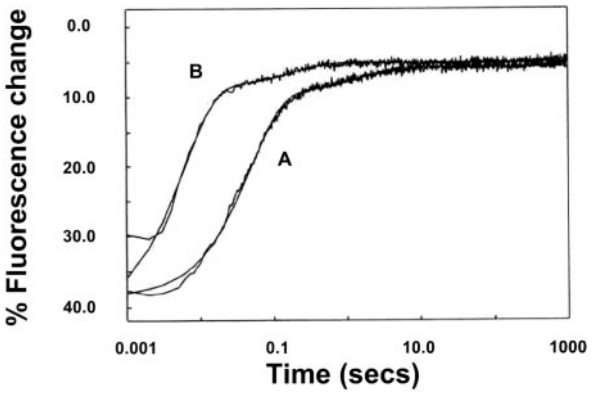


FIG. 7. **DTT induced dissociation of the ArsD-Sb(III) complex.** Two semi-logarithmic plots of stopped flow traces generated by mixing 1 $\mu$M ArsD/20 $\mu$M Sb(III) with 0.5 mM DTT (*trace A*) and 5.0 mM DTT (*trace B*). Changes in the ArsD fluorescence were recorded with excitation = 295 nm and emission > 335 nm. The *smooth curve* through the *traces* are the best fits to a double-exponential function, with rate constants of 20.0 ± 0.2 $s^{-1}$ (86% of total signal amplitude) and 0.55 ± 0.02 $s^{-1}$ (14% of total signal amplitude) for *trace A* and 166 ± 3 $s^{-1}$ (90% of total signal amplitude) and 5.2 ± 0.2 $s^{-1}$ (10% of total signal amplitude) for *trace B*. Both 0.5 and 5 mM DTT caused a 31–32% increase in fluorescence of ArsD-Sb(III).

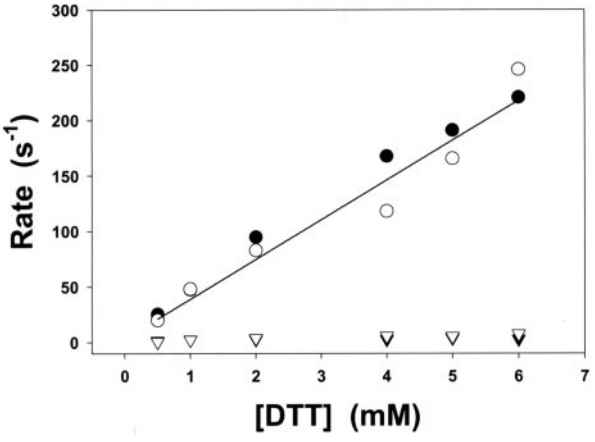


FIG. 8. **The concentration dependence of the DTT-induced dissociation of the ArsD-Sb(III) complex.** A series of stopped flow records were generated by mixing 1 $\mu$M ArsD/20 $\mu$M Sb(III) with DTT at the indicated concentrations in a stopped flow device. The rates of the fast and slow increase in the fluorescence of ArsD are plotted as a function of the DTT concentration. Two data sets are shown that were generated with ArsD (○, △) and C12A/C13A ArsD (●, ▲). The fast phase for ArsD and C12A/C13A ArsD increased in a linear manner, indicating second order rate constants of 36 ± 5 and 36 ± 1 $s^{-1}$ $\mu M^{-1}$, respectively.

tude) for *trace B*. Both 0.5 and 5 mM DTT caused a 31–32% increase in fluorescence of ArsD-Sb(III). The rate constant for the fast phase increased linearly with the DTT concentration, indicating a second order rate constant of 36 ± 5 $s^{-1}$ $\mu M^{-1}$, whereas that for the slow phase had little concentration dependence, suggestive of a conformational change in ArsD subsequent to Sb(III) dissociation (Fig. 8). Over the studied concentration range, of 0.1–5.0 mM DTT, the total signal amplitude was constant, indicating that all of the Sb(III), which could be sequestered by DTT, was displaced from the ArsD-Sb(III) complex. However, we note that the signal amplitude is slightly less than expected from the Sb(III)-induced quench in the ArsD fluorescence (*e.g.* 39% in stopped flow experiments), so that we cannot exclude the possibility that some Sb(III) remains bound to ArsD in the presence of DTT. The fact that the rate of DTT-induced dissociation of the ArsD-Sb(III) complex increases linearly with the DTT concentration is consistent with the dissociation process being rate limited by the collision or

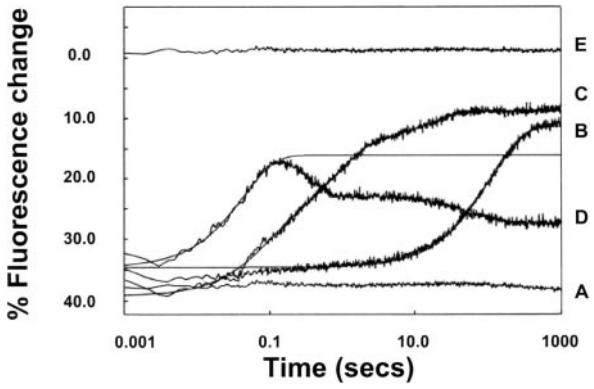


FIG. 9. **As(III)-induced dissociation of the ArsD-Sb(III) complex.** Five semi-logarithmic plots of stopped flow traces generated by mixing 1 $\mu$M ArsD/20 $\mu$M Sb(III) with buffer (*trace A*), 1 mM As(III) (*trace B*), 30 mM As(III) (*trace C*), 40 mM As(III) (*trace D*), and 1 $\mu$M ArsD mixed with buffer (*trace E*). *Trace B* was adequately defined by a single-exponential function, indicating a rate of 0.0091 ± 0.0001 $s^{-1}$, whereas *trace C* was more complex being best fitted to a triple exponential function that indicated rates of 14.5 ± 0.5, 1.50 ± 0.03, and 0.070 ± 0.002 $s^{-1}$. Because of the decrease in fluorescence that occurred after the first second of the reaction, only the fast phase of trace D could be analyzed, which indicated a rate of 23.1 ± 0.3 $s^{-1}$ when fitted to a single-exponential function.

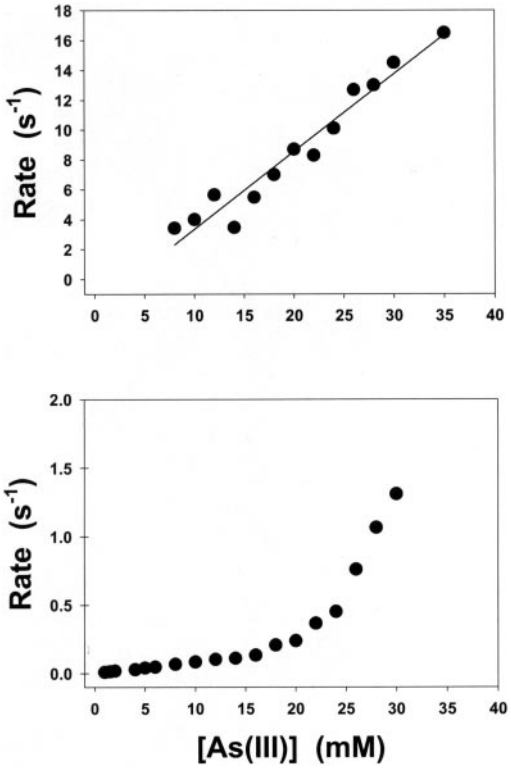


FIG. 10. **The concentration dependence of the As(III)-induced dissociation of the ArsD-Sb(III) complex.** A series of stopped flow records were generated by mixing 1 $\mu$M ArsD/20 $\mu$M Sb(III) with As(III), at the indicated concentrations, in a stopped flow device. The rates of the fast (*top panel*) and intermediate (*bottom panel*) increase in the fluorescence of ArsD are plotted as functions of the As(III) concentration. The rate of the fast phase increased in a linear manner, with a second-order rate constant of 0.52 ± 0.04 $mM^{-1}$ $s^{-1}$; although the maximal rate could not be defined, the rate of the intermediate phase clearly increased in a sigmoidal manner.

bimolecular association of DTT with the Sb(III)-ArsD complex. As discussed above, dissociation of Sb(III) from ArsD is too slow to be rate-limiting for this process, supporting our conclusion that Sb(III) is transferred directly from ArsD to bound DTT.

Steady-state studies revealed that the binding of Sb(III) to

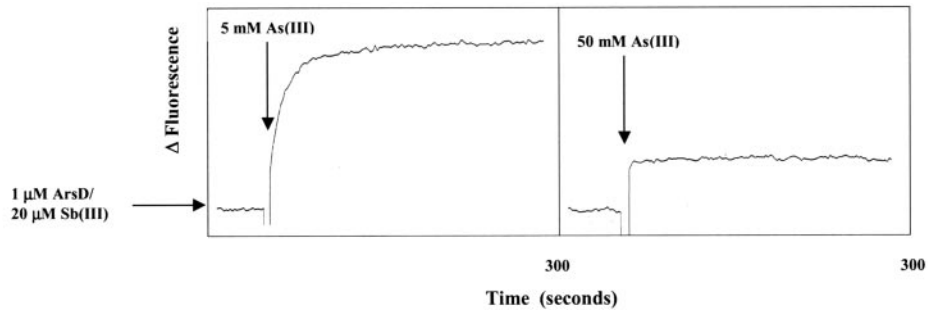


FIG. 11. **The As(III)-induced occlusion of Sb(III) bound to ArsD.** The time course for the displacement of Sb(III) from the ArsD-Sb(III) complex by As(III) was determined by manually adding 5 mM As(III) (*left panel*) and 50 mM As(III) (*right panel*) to 1 μM ArsD/20 μM Sb(III) in a stirred cuvette in a fluorimeter and monitoring the increase in protein fluorescence (excitation = 295 nm, emission = 340 nm) that resulted from the replacement of Sb(III) by As(III). The addition of 5 mM As(III) induced both rapid and slow release phases, whereas for the addition of 50 mM As(III), only the fast release phase was apparent. This behavior is consistent with As(III) replacing Sb(III) at one of the four metalloid-binding sites of ArsD, which then prevents Sb(III) release from the other three binding sites.

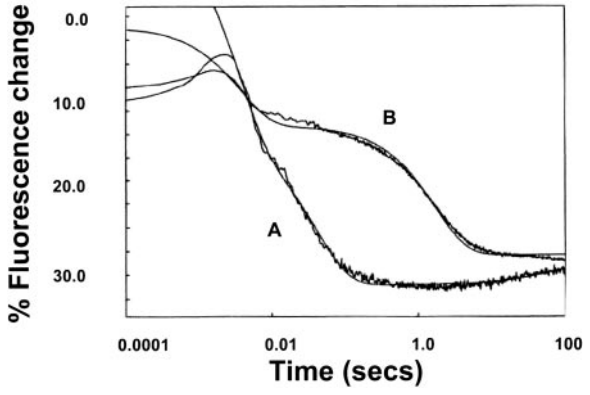


FIG. 12. **Sb(III)-induced conformational changes in C12A/C13A ArsD.** Two semi-logarithmic plots of stopped flow traces generated by mixing 120 μM Sb(III) with ArsD (*trace A*) and C12A/C13A ArsD (*trace B*). Changes in the protein fluorescence were recorded with excitation = 295 nm and emission > 335 nm. In the case of ArsD, the *smooth curve* through *trace A* was the best fit to a triple-exponential function, with rate constants of 290 ± 6, 24 ± 2, and 0.003 ± 0.001 $s^{-1}$. In the case of C12A/C13A ArsD, there was no intermediate binding phase as found for ArsD, and the data were adequately fitted to a biphasic exponential function with rate constants of 266 ± 5 $s^{-1}$ (43% of total signal amplitude) and 0.588 ± 0.005 $s^{-1}$ (57% of total signal amplitude).

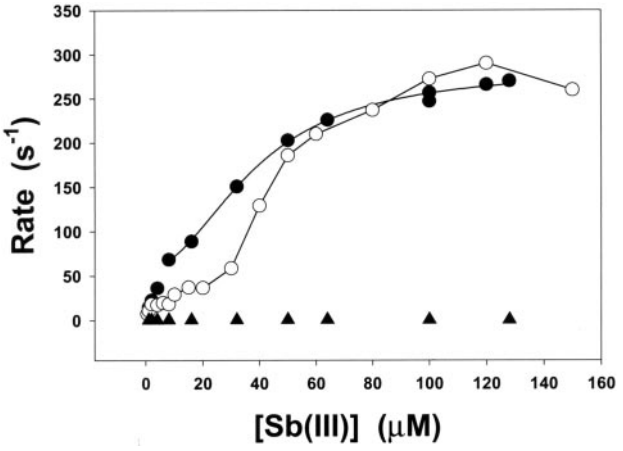


FIG. 13. **The Sb(III) concentration dependence of the rate of formation of the C12A/C13A ArsD-Sb(III) complex.** A series of stopped flow records were generated by mixing 1 μM C12A/C13A ArsD with Sb(III) at the indicated concentrations in a stopped flow device. The rates of the fast (●) and intermediate (▲) decrease in the fluorescence of C12A/C13A ArsD induced by the binding of Sb(III) are plotted as a function of the Sb(III) concentration. The rate constant for the fast phase increased in a sigmoidal manner, whereas that for the slow phase was apparently independent of the Sb(III) concentration. The curve through the data points for the fast phase is the best fit to a sigmoidal equation (Equation 2), indicating values for the Hill coefficients, $K_{1/2}$, $k_{max}$, and $k_{min}$ of 2.0 ± 0.3, 38 ± 2 μM, 225 ± 15 $s^{-1}$, and 59 ± 8 $s^{-1}$, respectively. The corresponding data for ArsD (○) are shown for comparison, illustrating the higher degree of cooperativity for ArsD in comparison with C12A/C13A ArsD.

ArsD produces about a 56% quench in the protein fluorescence, whereas As(III) causes only a 26% quench, allowing the displacement of Sb(III) by As(III) to be monitored as an increase in protein fluorescence (17). A couple of illustrative stopped flow traces are shown in Fig. 9 for the mixing of 1 μM ArsD/20 μM Sb(III) with 1 mM (*trace B*) and 30 mM (*trace C*) As(III). Although the total signal amplitude, measured as the difference between the initial and final fluorescence of ArsD in each trace, only increased from 27 to 31%, there was clearly a dramatic increase in the rate of Sb(III) displacement upon increasing the As(III) concentration from 1 to 30 mM. The trace for 1 mM As(III) was adequately defined by a single exponential function, indicating a rate of 0.0091 ± 0.0001 $s^{-1}$ (intermediate phase or phase 2), whereas the trace for 30 mM As(III) was more complex, being best fitted to a triple exponential function that indicated rates of 14.5 ± 0.5 $s^{-1}$ (fast phase 1, 24.7% of total amplitude), 1.50 ± 0.03 $s^{-1}$ (intermediate phase 2, 51.9% of total amplitude), and 0.070 ± 0.002 $s^{-1}$ (slow phase 3, 23.4% of total amplitude). The similarity in the total signal amplitudes for 1 and 30 mM As(III) and the fact that these values are comparable with the difference in the maximal fluorescence quenches for Sb(III) and As(III) (*e.g.* ~30%) indicate that both concentrations were sufficient to displace most of the bound Sb(III).

In view of these differences in the rate of displacement of Sb(III) by different concentrations of As(III), the As(III) concentration dependence of Sb(III) release from the ArsD-Sb(III) complex was examined. Both phase 1 and 3 were only well defined at the higher As(III) concentrations used, where these phases represented a reasonably substantial proportion of the total signal amplitude. Thus, for As(III) concentrations above 6 mM, the data were fitted to a triple exponential function, but below this concentration, the data were fitted to a single-exponential function. As shown in Fig. 10, the rate of phase 1 (Fig. 10, *top panel*) increased in an apparently linear manner with the As(III) concentration, whereas phases 2 (Fig. 10, *bottom panel*) and 3 (data not shown) increased in a sigmoidal manner. For As(III) concentrations above 30 mM, the amplitudes of phases 2 and 3 rapidly declined, and eventually these phases were replaced by a slow decrease in fluorescence (Fig. 9, *trace B*), making it impossible to obtain data at sufficiently high concentrations to define the maximal rates of phases 2 or 3. However, under such conditions the fast phase was still apparent (Fig. 9, *trace D*), and the rate of this phase was determined for concentrations as high as 200 mM As(III) ($k$ = 132 $s^{-1}$); no

deviation from a linear dependence was observed (data not shown). This behavior leads us to attribute this fast phase to the binding of As(III) to ArsD, which is rate-limited by the association of As(III) with ArsD, rather than by Sb(III) dissociation from ArsD. Furthermore, because the association of As(III) with the dissociating ArsD-Sb(III) complex was not rate-limited by the slow conformational change that rate limits As(III) association with unliganded ArsD (Fig. 6; $k_{max}$ = 8.7 $s^{-1}$), this suggests that dissociating Sb(III) leaves ArsD in a similar conformational state to that of the final ArsD-As(III) complex. In other words, there is rapid exchange of metalloids on ArsD. Interestingly, because the fast phase in the As(III)-induced dissociation of the ArsD-Sb(III) complex only accounts for about a quarter of the total signal amplitude, it is tempting to suggest that this phase corresponds to only one site. This would explain the disappearance of the intermediate and slow increase in fluorescence, which are replaced by a decrease in fluorescence for As(III) concentrations above 30 mM; the binding of As(III) to this fast exchange site induces a quench in the ArsD fluorescence that eventually overrides the increase in fluorescence because of Sb(III) release from the other sites. However, nearly saturating concentrations of As(III) only quench the fluorescence of ArsD by about 25%, whereas the maximum difference in the Sb(III) and As(III) quenches is about 30%. How then can As(III) binding to only one site override the increase in fluorescence because of Sb(III) release from the other sites? An alternative explanation might be that As(III) binding to the fast exchange site retards the release of Sb(III) from the other sites. To test this hypothesis 1 $\mu$M ArsD/20 $\mu$M Sb(III) was mixed with 5 and 50 mM As(III) in the fluorimeter; as expected, 5 mM As(III) induced a slow increase in fluorescence of about 35%, whereas 50 mM As(III) induced a rapid increase in fluorescence but of only about 10%, thus suggesting that 50 mM As(III) blocked the slow release of Sb(III) from ArsD (Fig. 11), which is consistent with the other sites only very slowly exchanging metalloids.

In common with the kinetics of As(III) binding to unliganded ArsD, the rate of phase 2 increased in a sigmoidal manner (Fig. 10, *bottom panel*). Moreover, this phase occurred at a rate similar to that for the binding of As(III) to unliganded ArsD (Fig. 6). However, although the rate of phase 2 was still increasing at concentrations above 30 mM As(III), the rate of binding of As(III) to unliganded ArsD had reached a saturable level with 30 mM As(III). This difference could easily be explained by the Sb(III) competing with the As(III) for binding to the remaining sites. Indeed, assuming simple competition, the $K_{½}$ for As(III) would increase from about 7 to 89 mM, *i.e.* the apparent $K_{d\ As(III)(app)} = K_{d\ As(III)} \cdot (1 + [Sb(III)]/K_{d\ Sb(III)})$, with a $K_{½}$ for Sb(III) of 1.7 $\mu$M and for As(III) of 7 mM, in the presence of 20 $\mu$M Sb(III)). Under these conditions, 30 mM As(III) would only give 25% saturation of the ArsD, and the rate of binding of As(III) should be about 2.2 $s^{-1}$, which is reasonably consistent with the measured value of 1.3 $s^{-1}$ (Fig. 10, *bottom panel*). We propose that, following the rapid binding of As(III) to the first unoccupied site, binding of As(III) to the remaining sites of ArsD is rate-limited by the same conformational change that rate limits As(III) association with unliganded ArsD.

*Characterization of the Kinetics of the Binding of Sb(III) to C12A/C13A ArsD*—To elucidate the origins of the cooperativity in metalloid binding to ArsD, the kinetics of the binding of Sb(III) to an ArsD substitution in which one of the binding sites had been disrupted by mutation of *arsD* was examined. For this analysis C12A/C13A ArsD was used because steady-state studies revealed that this protein was optically responsive to the binding of metalloids, whereas only small changes in the fluorescence of C112A/C113A ArsD were apparent, severely hindering detailed stopped flow fluorescence studies of this protein. The stopped flow traces for the binding of 120 $\mu$M Sb(III) to ArsD and C12A/C13A ArsD are compared in Fig. 12. In the case of C12A/C13A ArsD, there was no intermediate binding phase (*e.g.* phase 2) as found for ArsD, and the data were adequately fitted to a biphasic exponential function with rate constants of 266 ± 5 $s^{-1}$ (43% of total signal amplitude) and 0.588 ± 0.005 $s^{-1}$ (57% of total signal amplitude). In contrast to ArsD, only the fast phase of the binding of Sb(III) to C12A/C13A ArsD was characterized by a single concentration dependent phase, equivalent to phase 1 of the wild type, whereas phase 2 was clearly missing. These data suggest that phase 2 is attributable to metalloid binding to the $Cys^{12}$-$Cys^{13}$ site. The apparent rate of binding of Sb(III) to C12A/C13A ArsD increased in a sigmoidal manner but with less sigmoidicity than for ArsD (Fig. 13). As for the wild type, the first few data points deviated systematically from the best fit curve, consistent with our hypothesis that the fluorescence quench at these low concentrations is attributable to the initial filling of two of the sites, which must be the $Cys^{112}$-$Cys^{113}$ sites. As might be expected, a fit of the data points above 20 $\mu$M indicated a Hill coefficient of 2.0 ± 0.3, presumably because the $Cys^{12}$-$Cys^{13}$ sites are unavailable for metalloid binding.

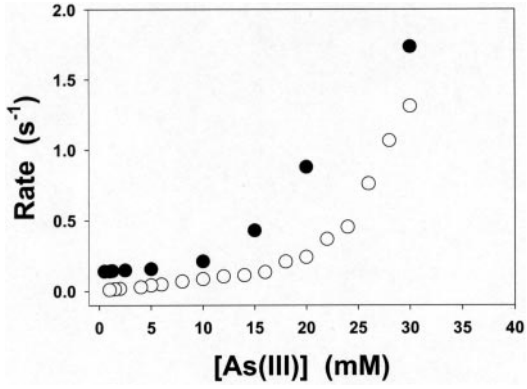


FIG. 14. **The concentration dependence of the As(III)-induced dissociation of the C12A/C13A ArsD-Sb(III) complex.** A series of stopped flow records were generated by mixing 1 $\mu$M C12A/C13A ArsD/20 $\mu$M Sb(III) with As(III), at the indicated concentrations, in a stopped flow device. The rate of the intermediate phase (●) for the increase in the fluorescence of C12A/C13A ArsD are plotted as a function of the As(III) concentration. Although the maximal rate could not be defined, the rate of the intermediate phase clearly increased in a sigmoidal manner. The corresponding data for ArsD (○) are shown for comparison, illustrating the titration curve for C12A/C13A ArsD is displaced to the left of that for ArsD.

The kinetics of the displacement of Sb(III) from C12A/C13A ArsD by DTT were identical to those for wild type ArsD (Fig. 8). In many respects the kinetics of Sb(III) displacement from C12A/C13A ArsD by As(III) also resembled those of the wild type but with two significant differences. First, the appearance of the decrease in protein fluorescence that overrides the As(III) induced increase in fluorescence occurs at much lower concentrations of As(III) (~10 mM as compared with 30 mM for the wild type). Consequently, none of the stopped flow traces for the increase in fluorescence induced by As(III) could be resolved into both fast and slow phases. Clearly though, for As(III) concentrations above 10 mM, there is a fast phase, because the rate of increase in protein fluorescence induced by As(III) is fast and increases linearly above this critical concentration (data not shown). Second, the concentration dependence curve for the slow phase is displaced to the left of that for the wild type (Fig. 14). The displacement of the data for C12A/C13A ArsD relative to that for ArsD might be attributed to the

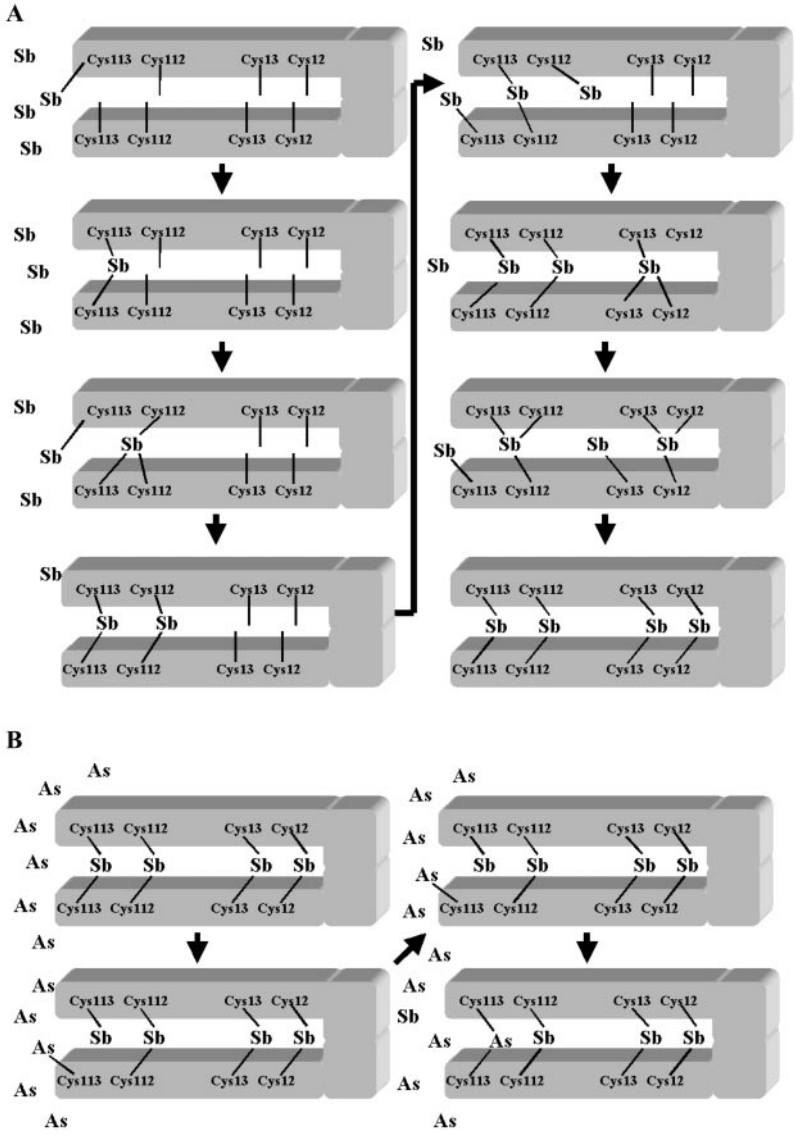


FIG. 15. **A model for metalloid binding to ArsD.** *A*, the metalloid-binding sites are composed of pairs of equivalent cysteine residues donated by each subunit of the ArsD dimer. The binding of metalloids, such as Sb(III), to the four binding sites occurs sequentially. The first Sb(III) is bound by the thiol side chains of the $Cys^{113}$ residues in each subunit. This Sb(III) can then be transferred to the next binding site, composed of the $Cys^{112}$ residues, and we envisage a transient state in which Sb(III) is bound by both $Cys^{113}$ and $Cys^{112}$ residues with either two or three protein ligands. This transfer of Sb(III) to the $Cys^{119}$ binding site releases the $Cys^{113}$ residues to bind another molecule of Sb(III). Subsequently the Sb(III) ions in the $Cys^{113}$ and $Cys^{112}$ binding sites can be transferred to the $Cys^{13}$ and $Cys^{12}$ binding sites. We propose that the ArsD dimer is closed to release Sb(III) from the latter sites and that dissociation is by a reversal of the above mechanism. *B*, As(III) can displace Sb(III) from the fast exchange $Cys^{113}$ binding site. For sufficiently high concentrations of As(III), the ArsD will in effect be saturated with As(III). In this state, the dissociation of As(III) from the $Cys^{113}$ site is improbable, and thus the release of Sb(III) from the other sites is prevented. The bonds between the thiol groups of the cysteine residues and the metalloids are shown as *straight lines*. Sb(III) and As(III) ions have been abbreviated to *Sb* and *As*, respectively.

Sb(III) competing less effectively with As(III) for binding to C12A/C13A ArsD than ArsD. However, 30 mM As(III) was insufficient to cause near saturation of C12A/C13A ArsD, whereas 10 mM As(III) was sufficient to cause near saturation of unliganded ArsD, suggesting that Sb(III) is still competing with As(III) for binding to C12A/C13A ArsD. A more plausible explanation for the displacement of the data for C12A/C13A ArsD relative to that for ArsD is to attribute this effect to a reduced degree of cooperativity in the binding of As(III) to C12A/C13A ArsD relative to that for ArsD.

## DISCUSSION

Although the mechanisms underlying the binding of *trans*-acting repressors to their target operator have been studied in detail, often identifying cooperativity in the binding process, there have been few detailed studies of the mechanisms of binding of inducers to these repressors that trigger the conformational changes that cause dissociation of the repressor from the operon. To date, the most detailed studies have been performed on the tetrameric LacI and dimeric TetR repressors, inserting tryptophan residues at defined positions within tryptophan-free derivatives and monitoring the exposure of these residues as the protein undergoes conformational changes induced by the binding of the inducer (18–21). These studies have been useful for elucidating the protein dynamics and in conjunction with structural data derived from x-ray crystallographic studies used to model the conformational changes that induce dissociation from the operon (22, 23). However, the conformational changes induced by the binding of the inducers have not been time-resolved, nor has any cooperativity between the inducer-binding sites been explored in those studies. Here the kinetics of binding of metalloids to ArsD and cooperativity between the metalloid-binding sites of ArsD, a *trans*-acting repressor of the *arsRDABC* operon that confers resistance to arsenicals and antimonials in *E. coli*, were examined.

In a previous study, *in vivo* assays of repression and induction and *in vitro* studies of DNA binding revealed that both the $Cys^{12}$-$Cys^{13}$ and $Cys^{112}$-$Cys^{113}$ pairs but not the $Cys^{119}$-$Cys^{120}$ pair were required for responses to metalloid inducers (17). Accordingly, experiments were designed to test whether these sites act independently in triggering the conformational changes in ArsD that induce it to dissociate from the operon. Titration of the protein fluorescence of ArsD (in which $Cys^{119}$ and $Cys^{120}$ had been deleted) revealed cooperativity in the binding process, which occurred with a Hill coefficient of 2. However, the binding of metalloids to a C12A/C13A substitution, constructed by further mutation of the C119/C120 ArsD deletion, was also cooperative, with a Hill coefficient of 2, indicating that cooperativity exists between the $Cys^{112}$-$Cys^{113}$

sites of adjacent ArsD monomers within the functional dimer. Consistent with this finding, C112A/C113A ArsD displayed little cooperativity, C12A/C13A/C112A ArsD was noncooperative, and C12A/C13A/C112A/C113A ArsD was unresponsive. On the other hand, the $Cys^{12}$-Cys13 pair is required for inducibility, suggesting that there are interactions between the two metalloid-binding sites within the ArsD monomer. The maximal fluorescence quench of C112A/C113A ArsD but not C12A/C13A ArsD was substantially reduced, indicating that the fluorescence changes are largely reporting on effects at the $Cys^{112}$-$Cys^{113}$ sites. Indeed, our previous studies indicated that, of the two tryptophans present in ArsD, $Trp^{35}$ and $Trp^{97}$, only $Trp^{97}$, which is presumably close to the $Cys^{112}$-$Cys^{113}$ site, reports metalloid binding to ArsD (17).

Stopped flow studies revealed that the binding of metalloids is a rapid process that is rate-limited by a change in the conformation of the ArsD-metalloid complex. Formation of this conformational state, which presumably has a lower affinity for the operon, is 25-fold faster for Sb(III) than As(III), consistent with Sb(III) being a better inducer. The rate of this conformational change increases as a function of Sb(III) concentration with a Hill coefficient of 4, indicating that all four binding sites of the dimer interact in a positive cooperative manner. Binding of Sb(III) to C12A/C13A ArsD was also rate-limited by a conformational change in the C12A/C13A ArsD-Sb(III) complex that occurred at a similar rate to that for ArsD. However, the binding process was characterized by a Hill coefficient of 2, consistent with the deletion of the $Cys^{12}$-$Cys^{13}$ sites within the dimer. Furthermore, although two concentration-dependent phases for the binding of Sb(III) to ArsD were apparent, only one concentration-dependent phase was apparent for C12A/C13A ArsD, suggesting that the second slow phase for ArsD is attributable to the binding of Sb(III) to the $Cys^{12}$-$Cys^{13}$ sites. Binding of Sb(III) to these sites induces a 10-fold slower conformational change in the ArsD-Sb(III) complex, which is presumably necessary for induction.

Interestingly, the binding sites behave differentially, with the replacement of Sb(III) by As(III) at one site rate-limited by the bimolecular association of As(III) with ArsD rather than by the subsequent conformational change in the ArsD-As(III) complex that rate limits the binding process at the other sites, but this behavior contrasts with that of DTT, which apparently induces rapid dissociation of bound Sb(III) from all the sites. Indeed, binding of As(III) to this so called fast exchange site occludes the Sb(III) from being replaced by As(III) at the other sites. Furthermore, the kinetics of the binding of Sb(III) indicates that at least one site must near saturation before the subsequent conformational changes in the ArsD-Sb(III) complex are triggered by binding of Sb(III) to the other sites. In these respects, this site can bind Sb(III) independently of the other sites and appears to play a regulatory role over the other sites. This site must be one of the $Cys^{112}$-$Cys^{113}$ sites within the dimer because similar kinetic behavior is noted for C12A/C13A ArsD, which lacks the $Cys^{12}$-$Cys^{13}$ sites. How can we account for this behavior? One possibility is that the binding sites fill and empty sequentially, as indicated by their positive cooperativity, because of metalloid exchange between the sites. We propose that As(III) is able to exchange with Sb(III) at the fast exchange site but that this blocks release from the other sites because the Sb(III) in these sites only dissociate by exchange with the fast exchange site, but this would be very slow because the other sites will have a higher affinity for metalloids because of the positive cooperativity (Fig. 15*A*). In other words, there is sequential exchange of the metalloids, with only the fast exchange site liberating free metalloid (Fig. 15*B*). Furthermore, to account for the cooperativity between the subunits of the ArsD dimer, which occurs with a Hill coefficient of 4, we propose that the binding sites are formed by and between the equivalent cysteine residues in each subunit (*i.e.* the $Cys^{113}$ residues in each subunit form a binding site). Indeed, the fact that a C112A/C13A/C12A substitution of ArsD, which only possesses one cysteine residue, can still bind metalloids implies that each monomer contributes a cysteine residue to each metalloid-binding site. In contrast, metalloid exchange can occur between each site and bound DTT, facilitating the rapid dissociation of metalloids from ArsD. Such exchange of metalloids between thiol-containing binding sites has been noted previously for both organic molecules (24) and proteins (25). Indeed, ArsD may be useful as a model in understanding how metal exchange occurs between proteins, such as between copper chaperones and their target proteins (26–28).

Apparently at odds with the simple role proposed for ArsD, that of primarily acting as an unliganded repressor that prevents the expression of ArsB at levels that become toxic for the cell, the present investigation has revealed a complex pattern of positive cooperativity between the metalloid-binding sites. One might have expected that negative cooperativity between these sites, with only the fully complexed protein being released from the operon, would have been more consistent with such a role. However, consider the isothermal curve for the formation of the initial complex that triggers the conformational change that presumably leads to induction (Fig. 4). The first site binds Sb(III) with a $K_{½}$ of about 10 $\mu$M, but full activation requires all the sites to be occupied (which is, in effect, negative cooperativity), and full activation occurs with a $K_{½}$ of about 44 $\mu$M. Furthermore, the isothermal curve for the C12A/C13A ArsD derivative, which only has two cooperating sites, is displaced to the left of the curve for ArsD (Fig. 13). Accordingly, although there is positive cooperativity in the binding of Sb(III) to ArsD, these interactions also cause the titration curve for formation of the initial complex to be displaced to the right, decreasing the overall affinity of ArsD for Sb(III) and increasing the concentration of Sb(III) needed for induction. These features of ArsD would be useful in allowing it to control the upper limit of expression of the operon. However, considering the tightness and capacity for binding metalloids by ArsD, it might play an additional role in buffering the free concentration of toxic metalloids within the cytoplasm and could conceivably act as a chaperone to deliver these metalloids to the pump.

REFERENCES


1. Dey, S., and Rosen, B. P. (1995) in *Drug Transport in Antimicrobial and Anticancer Chemotherapy* (Georgopapadakou, N. H., ed) pp. 103–132, Dekker, New York
2. Vulpe, C., Levinson, B., Whitney, S., Packman, S., and Gitschier, J. (1993) *Nat. Genet.* **3,** 7–13
3. Chelly, J., Tumer, Z., Tonnesen, T., Petterson, A., Ishikawa-Brush, Y., Tommerup, N., Horn, N., and Monaco A. P. (1993) *Nat. Genet.* **3,** 14–19
4. Mercer, J. F., Grimes, A., Ambrosini, L., Lockhart, P., Paynter, J. A., Dierick, H., and Glover, T. W. (1993) *Nat. Genet.* **3,** 20–25
5. Bull, P. C., Thomas, G. R., Rommens, J. M., Forbes, J. R., and Cox, D. W. (1993) *Nat. Genet.* **5,** 327–337
6. Tanzi, R. E., Petrukhin, K., Chernov, I., Pellequer, J. L., Wasco, W., Ross, B., Romano, D. M., Parano, E., Pavone, L., Brzustowicz, L. M., Devoto, M., Peppercorn, J., Bush, A. I., Sternlieb, I., and Piratsu, M. (1993) *Nat. Genet.* 5, 344–350
7. Chen, C. M., Misra, T. K., Silver, S., and Rosen, B. P. (1986) *J. Biol. Chem.* **261,** 15030–15038
8. Rosen, B. P., Bhattacharjee, H., Zhou, T., and Walmsley, A. R. (1999) *Biochim. Biophys. Acta* **1461,** 207–215
9. Oden, K. L., Gladysheva, T. B., and Rosen, B. P. (1994) *Mol. Microbiol.* **12,** 301–306
10. Gladysheva, T. B., Oden, K. L., and Rosen, B. P. (1994) *Biochemistry* **33,** 7287–7293
11. Liu, J., and Rosen, B. P. (1997) *J. Biol. Chem.* **272,** 21084–21089
12. Shi, J. Vlamis-Gardikas, A., Aslund, F., Holmgren, A., and Rosen, B. P. (1999) *J. Biol. Chem.* **274,** 36039–36042
13. Martin, P., DeMel, S., Shi, J., Gladysheva, T. B., Gatti, D. L., Rosen, B. P., and Edwards, B. F. P. (2001) *Structure Folding Design* **9,** 1071–1081

14. Xu, C., Shi, W., and Rosen, B. P. (1996) *J. Biol. Chem.* **271,** 2427–2432
15. Chen, Y., and Rosen, B. P. (1997) *J. Biol. Chem.* **272,** 14257–14262
16. Shi, W., Dong, J., Scott, R. A., Ksenzenko, M. Y., and Rosen, B. P. (1996) *J. Biol. Chem.* **271,** 9291–9297
17. Li, S., Chen, Y., and Rosen, B. P. (2001) *Mol. Microbiol.* **41,** 687–696
18. Barry, J. K., and Matthews, K. S. (1997) *Biochemistry* **36,** 15632–15642
19. Ozarowski, A, Barry, J. K., Matthews, K. S., and Maki, A. H. (1999) *Biochemistry* **38,** 6715–6722
20. Vergani, B., Kintrup, M., Hillen, W., Lami, H., Piemont, E., Bombarda, E., Alberti, P., Doglia, S. M., and Chabbert, M. (2000) *Biochemistry* **39,** 2759–2768
21. Kintrup, M., Schubert, P., Kunz, M., Chabbert, M., Alberti, P., Bombarda, E., Schneider, S., and Hillen, W. (2000) *Eur. J. Biochem.* **267,** 821–829
22. Matthews, K. S., Falcon, C. M., and Swint-Kruse, L. (2000) *Nat. Struct. Biol.* **7,** 184–187
23. Orth, P., Schnappinger, D., Hillen, W., Saenger, W., and Hinrichs, W. (2000) *Nat. Struct. Biol.* **7,** 215–219
24. Delnomdedieu, M., Basti, M. M., Otvos, J. D., and Thomas, D. J. (1993) *Chem. Res. Toxicol.* **6,** 598–602
25. Wernimont, A. K., Huffman, D. L., Lamb, A. L., O'Halloran, T. V., and Rosenzweig, A. C. (2000) *Nat. Struct. Biol.* **7,** 766–771
26. Harrison, M. D., Jones, C. E., Solioz, M., and Dameron, C. T. (2000) *Trends Biochem. Sci.* **25,** 29–32
27. Rosenzweig, A. C. (2001) *Acc. Chem. Res.* **34,** 119–128
28. Arnesano, F., Banci, L., Bertini, I., Ciofi-Baffoni, S., Molteni, E., Huffman, D. L., and O'Halloran, T. V. (2002) *Genome Res.* **12,** 255–271

**Evidence for Cooperativity between the Four Binding Sites of Dimeric ArsD, an As(III)-responsive Transcriptional Regulator**

Song Li, Barry P. Rosen, M. Ines Borges-Walmsley and Adrian R. Walmsley

*J. Biol. Chem. 2002, 277:25992-26002.*
*doi: 10.1074/jbc.M201619200 originally published online April 29, 2002*

---